An Interference Avoidance Code Assignment Strategy for Downlink Multi-Rate MC-DS-CDMA With TF-Domain Spreading

Li-Chun Wang, Chih-Wen Chang, and Howard Huang

***Abstract*— Frequency selective fading may affect the orthogonality of the spreading codes in the multi-carrier direct sequence code division multiple access (MC-DS-CDMA) systems. In this paper, we define a new performance metric called the multiple access interference (MAI) coefficient for the MC-DS-CDMA system to quantitatively predict the impact of inter-code interference with the time- and frequency-domain spreading in a frequency selective fading channel. With the help of MAI coefficient, a novel interference avoidance code assignment strategy is proposed. By jointly considering the incurred MAI effect and the blocking probability in the code tree structure, the proposed interference avoidance code assignment method can effectively reduce the MAI for the multi-rate MC-DS-CDMA system, while maintaining very good call blocking rate performance.**

***Index Terms*— Code assignment, interference avoidance, MAI coefficient, MC-DS-CDMA.**

I. Introduction

Multi-carrier direct sequence code division multiple access (MC-DS-CDMA) becomes an important transmission technique for the next generation broadband wireless services [1]–[4]. Thanks to the advantages of both multi-carrier transmission and spread-spectrum modulation, the MC-DS-CDMA system is more immune to dispersive fading, with a lower peak-to-average power ratio, and has more flexibility in designing a wireless system [5], [6]. From the radio resource management perspective, the MC-DS-CDMA system possesses another nice property of adjusting spreading gains in both the time and frequency domains to support versatile multi-rate services in different radio channel environments [7], [8].

To enhance the capacity of the MC-DS-CDMA system, the spectrum is shared by users with distinct codes in either time domain or frequency domain. Fig. 1 shows an example of an MC-DS-CDMA system with two-dimensional orthogonal variable spreading factor (OVSF) codes, where time- and frequency-domain spread gains are 8 and 4, respectively. In principle, the total spreading gain is equal to the product of the time domain spreading gain and the frequency domain spreading gain, and a combination of a time-domain code and a frequency-domain code is allocated to each user. Ideally, any two time-domain spreading codes without the ancestor and child relation in the OVSF code tree are orthogonal even with the same frequency-domain spreading code. Similarly, any two (even the same) time-domain spreading codes in two distinct frequency-domain code trees of Fig. 1 are orthogonal regardless of the ancestor and child relation.

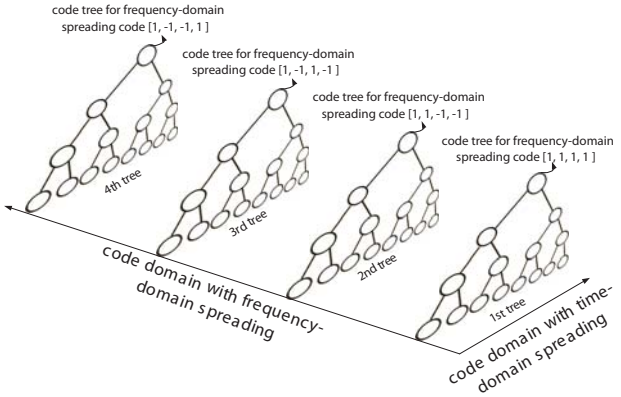

Fig. 1. A two-dimensional OVSF code tree when the frequency-domain spreading factor is four.

However, in a high-speed wireless system, the frequency-selective fading impairs the orthogonality of spreading codes. Thus, to reduce the impact of frequency-selective fading on the orthogonality of time-domain spreading codes, as shown in Fig. 4, the MC-DS-CDMA system adopts a serial-to-parallel process to convert a high speed data stream into multiple slower data streams. Thus, instead of frequency selective fading, it is the flat Rayleigh fading that influences the data in each subchannel after time-domain spreading. Hence, in the downlink case, the orthogonality between time-domain spreading codes can be maintained and the multiple access interference (MAI) of using the same frequency-domain spreading codes is eliminated. Nevertheless, frequency-selective fading can still affect the orthogonality of frequency-domain

Manuscript received November 11,2005; revised May 21, 2006 and November 12, 2006; accepted December 18, 2006. The associate editor coordinating the review of this paper and approving it for publication was D.-I. Kim. This work was supported jointly by the National Science Council and the Program of Promoting University Excellence of Ministry of Education, Taiwan, under the contracts 93-2219-E-009-012, 94-2213-E-009-060, 95-2218-E-006-041 and EX-91-E-FA06-4-4. Part of this work has been published in the IEEE International Conference on Communications, June 2006.

L.-C. Wang is with the Department of Communication Engineering, National Chiao Tung University, Taiwan Institute of Computer and Communication Engineering, National Cheng Kung University, Taiwan (e-mail: lichun@cc.nctu.edu.tw).

C.-W. Chang is with the Institute of Computer and Communication Engineering, National Cheng Kung University, No. 1 University Road, Tainan, 701 Taiwan (e-mail: cwchang@ee.ncku.edu.tw).

H. Huang is with Alcatel-Lucent Technologies, 791 Holmdel-Keyport Rd., Holmdel, NJ 07733 USA (e-mail: hchuang@alcatel-lucent.com).

Digital Object Identifier 10.1109/TWC.2007.xxxxx.

spreading codes. In a multi-rate MC-DS-CDMA system, the imperfect orthogonality of frequency-domain spread codes even cause different amplitudes of MAI due to various transmit power levels for supporting multi-rate services.

Accordingly, a challenging issue arises: how can an MC-DS-CDMA system effectively assign a combination of frequency- and time-domain spreading codes for multi-rate users to avoid different amplitudes of MAI in a frequency selective fading channel. Another important concern for code assignment is to sustain the compactness of the tree structure of the OVSF codes for improving the call blocking performance. In this paper, we propose an interference avoidance code assignment strategy to consider both the MAI and call blocking performance simultaneously. The proposed interference avoidance code assignment strategy can reuse spreading codes in both the time and frequency domains to enhance capacity, while controlling the incurred MAI due to reusing the time-domain spreading codes. The key to the proposed interference avoidance code assignment scheme is the newly defined performance metric — the *MAI coefficient*, which can quantitatively predict the incurred MAI before assigning a particular code. By choosing a code with the minimum incurred MAI in the multi-rate multiuser MC-DS-CDMA system, the signal quality can be improved significantly. Furthermore, the proposed code assignment strategy sustains the compactness of the code tree structure, thereby achieving very good call blocking rate performance. The literature survey for other code assignment techniques will be discussed in the next section.

The rest of this paper is organized as follows. In Section II, we provide a literature survey and introduce the two-dimension OVSF code tree structure in the MC-DS-CDMA system with time and frequency domain spreading. In Section III, we introduce the signal model and analyze the MAI of the MC-DS-CDMA system. In Section IV, we define the performance metric — *MAI coefficient*. In Section V proposes an interference avoidance code assignment strategy for the multi-rate MC-DS-CDMA system with TF-domain spreading. Numerical results are provided in Section VI. We give our concluding remarks in Section VII.

II. Literature Survey and Problem Formulation

A. Literature Survey

In the literature, most code assignment techniques in the single carrier CDMA system were proposed without considering the impact of MAI. In [9]–[11], code assignment techniques were investigated with an aim to keep the code tree compact for the purpose of reducing the call blocking rate and the code reassignments in the single carrier CDMA system with OVSF codes. To eliminate the MAI in asynchronous MC-DS-CDMA, the interference-rejection and interference-free spreading codes were proposed in [12] and [13], respectively. In [14], [15], the authors proposed a code assignment strategy based on the dual quasi-orthogonal and Walsh codes to reduce the MAI in the MC-DS-CDMA systems. In [16], an MAI-minimized signature waveforms was proposed to minimize the MAI for the MC-DS-CDMA systems. In the above MC-DS-CDMA systems, [12]–[16] all belong to MC-DS-CDMA with one-dimensional time-domain spreading.

For the MC-DS-CDMA system with time- and frequency-domain spreading, the authors in [8] proposed a novel two-dimension (2D) OVSF codes with good properties of zero autocorrelation sidelobes and the zero cross-correlation functions. By changing the time- and frequency-domain spreading factors, the 2D OVSF codes in [8] can support multi-rate transmissions. However, the frequency diversity gain of the above mentioned 2D OVSF codes becomes different when transmitting signals at various data rates. One should note that the 2D OVSF codes in [8] and our proposed scheme, as shown in Fig. 1, can provide the same number of spreading codes for downlink transmission.

In this paper, we consider a downlink MC-DS-CDMA system with a constant frequency diversity gain. Furthermore, we investigate the MAI impact caused by reusing time-domain spreading codes in the MC-DS-CDMA, which is not considered in [8], [12]–[16].

B. Two-Dimensional OVSF Code Tree Structure for the MC-DS-CDMA System

In the multi-rate MC-DS-CDMA system with TF-domain spreading, the OVSF code tree has a two-dimensional structure, as shown in Fig. 1. In the figure, the frequency-domain spreading factor is four and the time-domain spreading factor ranged between 1 to 8 depending on the requested data rates by users. The OVSF spreading code in either time domain or frequency domain can be constructed according to the rule of the one-dimension OVSF code [17]. Now we discuss the orthogonality of the codes in the two dimension OVSF code tree. To easy the illustration, we spread the 2-D code tree in Fig. 1 onto a plane as in Fig. 2. In the two-dimension OVSF code tree shown in Fig. 1, the total spreading factor is equal to $SF_f \times SF_t$, where $SF_f = 4$ is the frequency domain spreading factor and $SF_t = 1 \sim 8$ is the time-domain spreading factor, respectively. Thus, an OVSF code tree with the maximum spreading factor of 8 is copied four times for each associated frequency-domain spreading code. Denote $C^{(i)}_{2^{l-1},n}$ $(n = 1, \ldots, 2^{(l-1)})$ the n-th code of the code group in the l-th layer associated with the i-th code tree, where the time-domain spreading factor $SF_t = 1 \sim 2^{(l-1)}$ from the top layer ($l = 1$) to the bottom layer ($l = 4$) of the OVSF code tree. Ideally, any two codes in two frequency-domain code trees are orthogonal due to the orthogonal frequency-domain spreading codes. However, due to the frequency-selective fading, this condition may no longer be true. We say that two codes in the two dimensional OVSF code tree are *related codes* if they have an ancestor-descendant relationship in the time domain. For example, $C^{(1)}_{4,1}$=[1 1 1 1] and $C^{(2)}_{8,1}$=[1 1 1 1 1 1 1 1]) are related codes, where $C^{(1)}_{4,1}$ and $C^{(2)}_{8,1}$ are associated with the frequency-domain spreading codes [1 1 1 1] and [1 1 -1 -1], respectively. Note that $C^{(1)}_{4,1}$ will interfere $C^{(2)}_{8,1}$ and vice versa.

C. Grid Representation of a 2-D Code Tree

First, we introduce a grid representation of the code resource for the MC-DS-CDMA system with the time- and frequency-domain two-dimensional spreading. In the grid representation, the code resources are illustrated by a set of

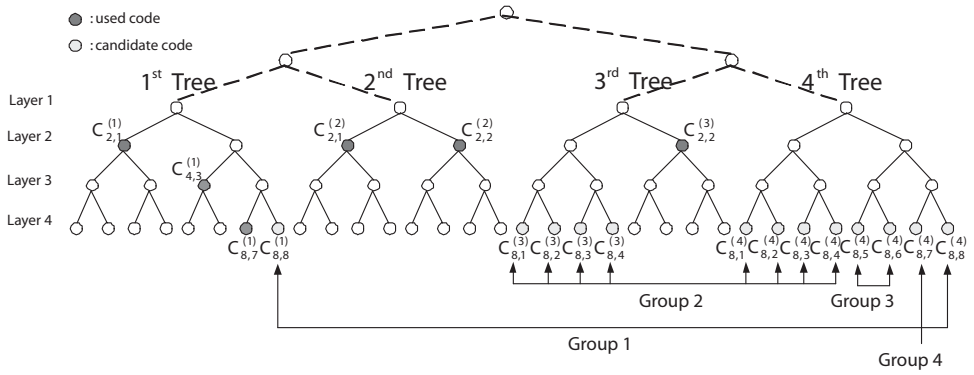

Fig. 2. An illustrating example of allocating a code with frequency-domain spreading factor $M = 4$ and time-domain spreading factor $SF = 8$ in the 2D code tree.

rectangles. Code channels with the same spreading factor SF_t can be represented by a set of equal-sized rectangles. The area of each rectangle is proportional to the transmission rate of the corresponding code channel (or inversely proportional to SF_t). For the 2-D code tree of Fig. 2 with some allocated codes, the corresponding grid representation of available codes is shown in Fig. 3. In Figs. 2 and 3, the dark and the gray circles (squares) stand for the "used code" and "candidate code" with a requested code of SFt = 8, respectively. As shown in Fig. 3, the code channels with $SF_t = 2$ at layer 2 are represented by a set of the largest equal-sized rectangles while code channels with $SF_t = 8$ at layer 4 are represented by the smallest equal-sized rectangles, each of which is sized up to one quarter of the size of a rectangle with $SF_t = 2$. The plot at the bottom of Fig. 3, an aggregate of the blocks of layer 2∼4 summarizes the total used and free code resources. Now, with the aid of the grip representation, we can clearly define the related codes as:

$$\textit{Related Codes} \equiv \textit{The used codes positioned in the same column of the grip representation} \quad (1)$$

For example, $\{C_{8,8}^{(1)}, C_{2,2}^{(2)}, C_{2,2}^{(3)}, C_{8,8}^{(4)}\}$ seated in the most right column is a set of related codes. One should note that codes belong to the same set of related codes can interfere with each other.

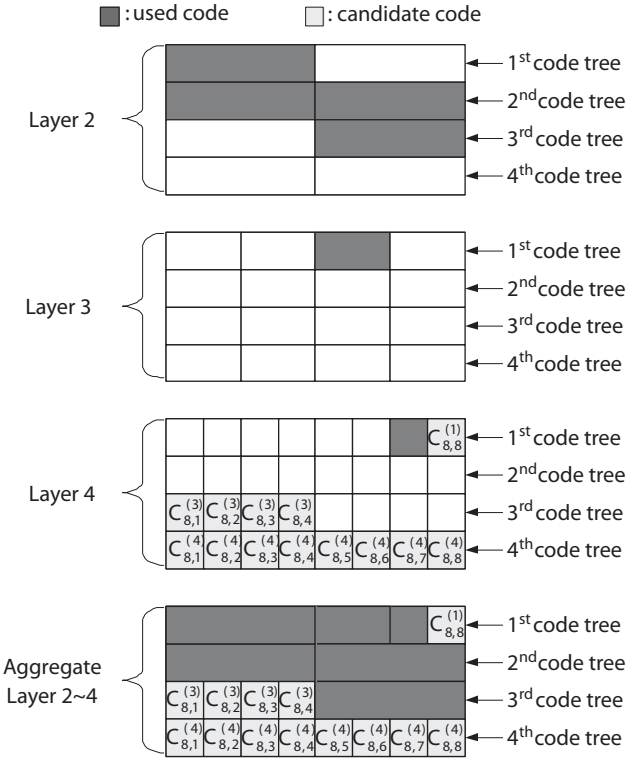

Fig. 3. The grid representation of Fig. 2 for the code resources in the MC-DS-CDMA system with time and frequency domain spreading.

D. Motivation

Consider a scenario when a code with time-domain spreading factor $SF = 8$ is requested. Clearly, the candidate codes for this request are $\{C_{8,8}^{(1)}, C_{8,1}^{(3)}, C_{8,2}^{(3)}, C_{8,3}^{(3)}, C_{8,4}^{(3)}, C_{8,1}^{(4)}, C_{8,2}^{(4)}, C_{8,3}^{(4)}, C_{8,4}^{(4)}, C_{8,5}^{(4)}, C_{8,6}^{(4)}, C_{8,7}^{(4)}, C_{8,8}^{(4)}\}$. According to the interferers of the allocated codes by observing the grid representation in Fig. 3, these candidate codes can be roughly classified into four groups as shown in Fig. 2. Specifically, Groups 1 to 4 are affected by the interference from the users with the allocated codes $\{C_{2,2}^{(2)}, C_{2,2}^{(3)}\}$, $\{C_{2,1}^{(1)}, C_{2,1}^{(2)}\}$, $\{C_{4,3}^{(1)}, C_{2,2}^{(2)}, C_{2,2}^{(3)}\}$, and $\{C_{8,7}^{(1)}, C_{2,2}^{(2)}, C_{2,2}^{(3)}\}$, respectively.

Then, an interesting question arise: how can an MC-DS-CDMA system pick a code from a 2-D code tree with less MAI, while maintaining a compact code tree structure to further achieve a lower call blocking probability? More importantly, the *potential* impact on the existing used codes should be taken into account for evaluating the candidacy of a code. There are two main challenges. First, the impact of the incurred MAI for a candidate code should be *predicted* before transmitting a signal. This MAI prediction scheme should not only be accurate but simple. Second, multi-rate users make the code assignment problem nontrivial since some high-rate users may request more channel resources. Thus, a 2-D code tree structure should be considered in the code assignment problem aiming to reduce the call blocking rate for multi-rate users.

Hence, we are motivated to propose a new performance metric, called the *MAI coefficient*, to quantitatively estimate the amount of the possible incurred MAI for the candidate codes. Moreover, based on the newly defined *MAI coefficient*, we propose a novel interference avoidance code assignment strategy for MC-DS-CDMA with time- and frequency-domain spreading, which can effectively reduce the impact of MAI and achieve low call blocking performance.

III. System Model

A. Transmitted Signal

The transmitter structure in the MC-DS-CDMA system using both time- and frequency-domain spreading codes is shown in Fig. 4. First, the serial-to-parallel process reduces the subcarrier data rate by converting data streams with bit duration $T_{b,k}^{(\mathbf{X})}$ into U reduced-rate parallel substreams with new bit duration $T_k^{(\mathbf{X})} = UT_{b,k}^{(\mathbf{X})}$ for user k in group $\mathbf{X} \in \{\mathbf{A}, \mathbf{B}, \mathbf{C}\}$, where each substream experiences a frequency flat (or non-dispersive) fading. Then the data in each substream are spread by a time domain spreading code $g_k^{(\mathbf{X})}(t)$. After being copied to M subcarriers, the data in each substream is multiplied by a frequency-domain spreading code $\{c_k^{(\mathbf{X})}[j]\}$. Note that in this case the frequency-domain spreading gain is M. The user group $\mathbf{X}$ is defined as follows. Let $g_o(t)$ and $c_o[j]$ be the time domain spreading code and the frequency-domain spreading code of the reference user, respectively. In principle, any two users should at least use one orthogonal spreading code in either time or frequency domain to distinguish from one to another. Therefore, similar to [7], we categorize the interfering users into three groups:

$$\text{(1) group } \mathbf{A}: \begin{cases} \dfrac{1}{T_o}\displaystyle\int_0^{T_o} g_k^{(\mathbf{A})}(t)g_o(t)dt \neq 0 \\ \dfrac{1}{M}\displaystyle\sum_{j=1}^{M} c_k^{(\mathbf{A})}[j]c_o[j] = 0 \end{cases},$$

$$\text{(1) group } \mathbf{B}: \begin{cases} \dfrac{1}{T_o}\displaystyle\int_0^{T_o} g_k^{(\mathbf{B})}(t)g_o(t)dt = 0 \\ \dfrac{1}{M}\displaystyle\sum_{j=1}^{M} c_k^{(\mathbf{B})}[j]c_o[j] \neq 0 \end{cases},$$

$$\text{(1) group } \mathbf{C}: \begin{cases} \dfrac{1}{T_o}\displaystyle\int_0^{T_o} g_k^{(\mathbf{C})}(t)g_o(t)dt = 0 \\ \dfrac{1}{M}\displaystyle\sum_{j=1}^{M} c_k^{(\mathbf{C})}[j]c_o[j] = 0 \end{cases}.$$

One should note that the above grouping of users is only valid for the downlink MC-DS-CDMA system. Also, group A will disappear and groups B and C will be blended into one group when using a single frequency-domain spreading code with all chips equal to one for all users. In that case, the system capacity will be largely reduced.

The transmitted signal of user k in group $\mathbf{X} \in \{\mathbf{A}, \mathbf{B}, \mathbf{C}\}$ can be expressed as

$$s_k^{(\mathbf{X})}(t) = \sum_{i=1}^{U}\sum_{j=1}^{M}\sqrt{\frac{2P_k^{(\mathbf{X})}}{M}}b_{k,i}^{(\mathbf{X})}(t)g_k^{(\mathbf{X})}(t)c_k^{(\mathbf{X})}[j] \times \cos(2\pi f_{i,j}t + \varphi_{k,i,j}^{(\mathbf{X})}) \ , \quad (2)$$

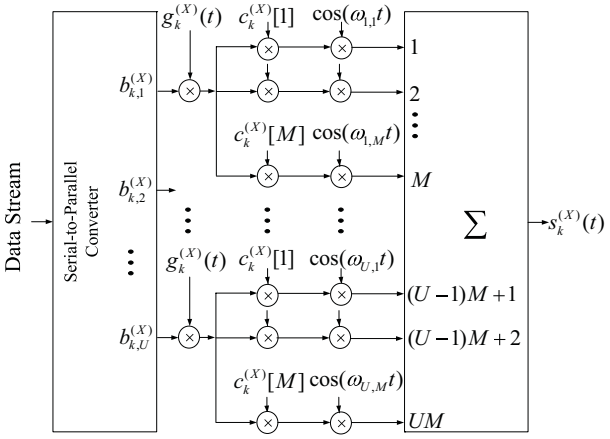

Fig. 4. The transmitter structure of the MC-DS-CDMA using time- and frequency-domain spreading codes.

where $P_k^{(\mathbf{X})}$, $\{f_{i,j}\}$ and $\{\varphi_{k,i,j}^{(\mathbf{X})}\}$ represent the transmitted power, the j-th subcarrier frequency and the initial phase in the i-th substream, respectively. Note that as in [18], the spectrum of the considered MC-DS-CDMA system is overlapped and any two adjacent subcarriers are separated by a minimum distance to preserve the orthogonality in the frequency domain. The waveform of the i-th substream $b_{k,i}^{(\mathbf{X})}(t) = \sum_{h=-\infty}^{\infty} b_{k,i}^{(\mathbf{X})}[h]P_{T_k^{(\mathbf{X})}}(t - hT_k^{(\mathbf{X})})$ contains a rectangular pulses of duration $T_k^{(\mathbf{X})}$, where $b_{k,i}^{(\mathbf{X})}[h] = \pm 1$ with equal probability. The time domain spreading code $g_k^{(\mathbf{X})}(t) = \sum_{\ell=-\infty}^{\infty} g_k^{(\mathbf{X})}[\ell]P_{T_c}(t - \ell T_c)$ represents the chip sequence of the rectangular pulses of duration T_c, where $g_k^{(\mathbf{X})}[\ell] = \pm 1$ with equal probability. Note that the time domain spreading factor of user k in the group $\mathbf{X}$ is $G_k^{(\mathbf{X})} = T_k^{(\mathbf{X})}/T_c$.

B. Received Signal

The impact of non-orthogonality of time- and frequency-domain spreading codes in the frequency selective fading channel will cause the multi-access interference on the received signal. Consider the downlink transmission in a single cell without power control and assume that each subcarrier experiences the flat Rayleigh fading. In such an environment, this kind of MAI will impact the desired user via the desired user's propagation path. Thus, the amount of path loss and fading of the multi-access interference will be equal to that of the the reference user. Thus, similar to [14]–[16], the impact of path loss is neglected in the analytical model for simplicity. Then, the received signal of the reference user (denoted by r_o) can be expressed as:

$$r_o(t) = \sum_{i=1}^{U}\sum_{j=1}^{M}\sqrt{\frac{2P_o}{M}}\alpha_{i,j}b_{o,i}(t)g_o(t)c_o[j]\cos(2\pi f_{i,j}t + \phi_{i,j}) + \sum_{\mathbf{X}\in\{\mathbf{A},\mathbf{B},\mathbf{C}\}}\sum_{k=1}^{K_{\mathbf{X}}}\sum_{i=1}^{U}\sum_{j=1}^{M}\sqrt{\frac{2P_k^{(\mathbf{X})}}{M}}\alpha_{i,j}b_{k,i}^{(\mathbf{X})}(t)g_k^{(\mathbf{X})}(t) \times c_k^{(\mathbf{X})}[j]\cos(2\pi f_{i,j}t + \phi_{i,j}) + n(t) \ , \quad (3)$$

where $\alpha_{i,j}$ is the channel amplitude for the j-th subcarrier of the i-th substream; $K_{\mathbf{X}}$ is the number of users in the group

$\mathbf{X}$; and $n(t)$ is the white Gaussian noise with double-sided power spectrum density of $N_0/2$. In (3), $\phi_{i,j} = \varphi_{i,j} + \psi_{i,j}$ is uniformly distributed in $[0, 2\pi)$, where $\psi_{i,j}$ is the channel's phase of the i-th subcarrier in the j-th substream. As in [18], [19], the subcarriers carrying the same data bit ($\alpha_{i,1} \sim \alpha_{i,M}$) are assumed to experience independent flat Rayleigh fading channels.

The receiver structure of the MC-DS-CDMA using time-domain and frequency-domain spreading codes is shown in Fig. 5. Without loss of generality, let the bit of interest be the first bit in the s-th substream of the reference user (denoted by $b_{o,s}[0]$). After time domain despreading, the output signal for the reference user in the v-th subcarrier of the s-th substream can be expressed as:

$$\begin{aligned} Y_{o,s,v} &= \int_0^{T_o} r_o(t)\beta_{s,v}g_o(t)c_o[v]\cos(2\pi f_{s,v}t + \phi_{s,v})dt \\ &= \sqrt{\frac{P_o}{2M}}T_o \left\{ b_{o,s}[0]\alpha_{s,v}\beta_{s,v} + \sum_{\mathbf{X}\in\{\mathbf{A},\mathbf{B},\mathbf{C}\}} \sum_{k=1}^{K_{\mathbf{X}}} I_{k,s,v}^{(\mathbf{X})} + \right. \\ &\quad \left. n_{s,v} \right\} \ , \end{aligned} \tag{4}$$

where P_o and T_o are the transmitted power and the bit duration of the reference user, respectively; $\beta_{s,v}$ is the weights for a certain combining scheme; $I_{k,s,v}^{(\mathbf{X})}$ denotes the MAI induced from user k of group $\mathbf{X}$ to the v-th subcarrier of the s-th substream of the reference user; and $n_{s,v}$ is the white Gaussian noise with zero mean and variance of $\frac{|\beta_{o,s,v}|^2}{2}(\frac{E_o}{MN_0})^{-1}$, where $E_o = P_oT_o$ is the bit energy of the reference user. The MAI terms $I_{k,s,v}^{(\mathbf{X})}$ in (4) can be expressed as

$$\begin{aligned} I_{k,s,v}^{(\mathbf{X})} &= \sqrt{\frac{P_k^{(\mathbf{X})}}{P_o}} \frac{\alpha_{s,v}\beta_{s,v}c_k^{(\mathbf{X})}[v]c_o[v]}{T_o} \int_0^{T_o} b_{k,s}^{(\mathbf{X})}(t) \times \\ &\quad g_k^{(\mathbf{X})}(t)g_o(t)dt \ . \end{aligned} \tag{5}$$

Then combining M subcarriers, the decision variable of $b_{o,s}[0]$ for the reference user becomes

$$Y_{o,s} = \sum_{v=1}^{M} Y_{o,s,v} \ , \tag{6}$$

where $Y_{o,s,v}$ is given in (4).

IV. Impact of MAI

In this section, we analyze the effect of MAI in the multi-rate MC-DS-CDMA system. To calculate $I_{k,s,v}^{(\mathbf{X})}$, we need to further consider two scenarios according to the relation between T_o (the bit duration of the reference user) and $T_k^{(\mathbf{X})}$ (the bit duration of the interfering user k in group $\mathbf{X}$).

A. *MAI From High Data Rate Users* ($T_o > T_k^{(\mathbf{X})}$) :

In this case, we let $L_k^{(\mathbf{X})} = T_o/T_k^{(\mathbf{X})}$ be the ratio of bit duration of the desired users to the interfering user of group $\mathbf{X} \in \{\mathbf{A}, \mathbf{B}, \mathbf{C}\}$, where $L_k^{(\mathbf{X})}$ is a positive integer. Then we

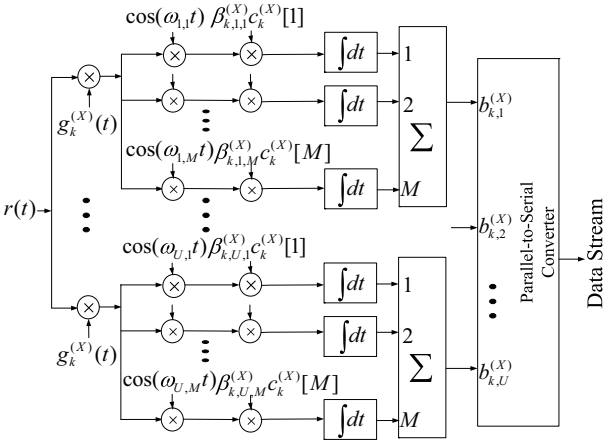

Fig. 5. The receiver structure of the MC-DS-CDMA using time- and frequency-domain spreading codes.

can rewrite (5) as

$$\begin{aligned} I_{k,s,v}^{(\mathbf{X})} &= \sqrt{\frac{P_k^{(\mathbf{X})}}{P_o}} \frac{\alpha_{s,v}\beta_{s,v}c_k^{(\mathbf{X})}[v]c_o[v]}{T_o} \int_0^{T_o} b_{k,s}^{(\mathbf{X})}(t)g_k^{(\mathbf{X})}(t)g_o(t)dt \\ &= \sqrt{\frac{P_k^{(\mathbf{X})}}{P_o}} \frac{\alpha_{s,v}\beta_{s,v}c_k^{(\mathbf{X})}[v]c_o[v]}{L_k^{(\mathbf{X})}T_k^{(\mathbf{X})}} \sum_{\ell=0}^{L_k^{(\mathbf{X})}-1} b_{k,s}^{(\mathbf{X})}[\ell] \times \\ &\quad \int_0^{T_k^{(\mathbf{X})}} g_k^{(\mathbf{X})}(t)g_o(t)dt \ . \end{aligned} \tag{7}$$

According to the definition of user group in Section II-A, the time-domain spreading codes of users in groups $\mathbf{B}$ and $\mathbf{C}$ are orthogonal to the reference user, i.e. $\int_0^{T_k^{(\mathbf{B})}} g_k^{(\mathbf{B})}(t)g_o(t)dt = 0$ and $\int_0^{T_k^{(\mathbf{C})}} g_k^{(\mathbf{C})}(t)g_o(t)dt = 0$. Hence, we have $I_{k,s,v}^{(\mathbf{B})} = I_{k,s,v}^{(\mathbf{C})} = 0$. Recall that $b_{k,s}^{(\mathbf{C})}[\ell] = \pm 1$ with equal probability. Thus, for OVSF codes, we can have

$$\frac{b_{k,s}^{(\mathbf{C})}[\ell]}{T_k^{(\mathbf{A})}} \int_0^{T_k^{(\mathbf{A})}} g_k^{(\mathbf{A})}(t)g_o(t)dt = \pm 1 \tag{8}$$

with equal probability. Consequently, (7) can be expressed as

$$I_{k,s,v}^{(\mathbf{A})} = \sqrt{\frac{P_k^{(\mathbf{A})}}{P_o}} \frac{\alpha_{s,v}\beta_{s,v}c_k^{(\mathbf{A})}[v]c_o[v]}{L_k^{(\mathbf{A})}} \sum_{\ell=0}^{L_k^{(\mathbf{A})}-1} \Delta[\ell] \ , \tag{9}$$

where $\Delta[\ell] = \pm 1$ with equal probability.

B. *MAI From Low Data Rate Users* ($T_o \le T_k^{(\mathbf{X})}$) :

In this case, we express $I_{k,s,v}^{(\mathbf{X})}$ as

$$\begin{aligned} I_{k,s,v}^{(\mathbf{X})} &= \sqrt{\frac{P_k^{(\mathbf{X})}}{P_o}} \frac{\alpha_{s,v}\beta_{s,v}c_k^{(\mathbf{X})}[v]c_o[v]}{T_o} \int_0^{T_o} b_{k,s}^{(\mathbf{X})}(t)g_k^{(\mathbf{X})}(t)g_o(t)dt \\ &= \sqrt{\frac{P_k^{(\mathbf{X})}}{P_o}} \frac{\alpha_{s,v}\beta_{s,v}c_k^{(\mathbf{X})}[v]c_o[v]}{T_o} b_{k,s}^{(\mathbf{X})}[0] \times \\ &\quad \int_0^{T_o} g_k^{(\mathbf{X})}(t)g_o(t)dt \ . \end{aligned} \tag{10}$$

Similar to the case of MAI from high data rate users, we have $I_{k,v}^{(\mathbf{B})} = I_{k,v}^{(\mathbf{C})} = 0$ and

$$\frac{b_{k,s}^{(\mathbf{X})}[0]}{T_o} \int_0^{T_o} g_k^{(\mathbf{A})}(t)g_o(t)dt = \pm 1 \ . \tag{11}$$

It follows that

$$I_{k,s,v}^{(\mathbf{A})} = \sqrt{\frac{P_k^{(\mathbf{A})}}{P_o}}\alpha_{s,v}\beta_{s,v}c_k^{(\mathbf{A})}[v]c_o[v]\Delta[0] \ , \quad (12)$$

where $\Delta[0]$ is defined in (9). Note that (12) is the special case of (9). Specifically, we can obtain (12) by letting $L_k^{(\mathbf{A})} = 1$ in (9).

Assuming maximum ratio combining, the combining weights are given by $\beta_{s,v} = \alpha_{s,v}^*$. Substituting (4), (9), and (12) into (6), we obtain

$$\begin{aligned} Y_{o,s} &= \sum_{v=1}^{M} Y_{o,s,v} \\ &= \sqrt{\frac{P_o}{2M}}T_o \left\{ b_{o,s}[0]\sum_{v=1}^{M}|\alpha_{s,v}|^2 + \sum_{v=1}^{M}\sum_{k=1}^{K_{\mathbf{A}}}\sum_{\ell=0}^{L_k^{(\mathbf{A})}-1} \right. \\ &\quad \left. \sqrt{\frac{P_k^{(\mathbf{A})}}{P_o}}\frac{|\alpha_{s,v}|^2 c_k^{(\mathbf{A})}[v]c_o[v]}{L_k^{(\mathbf{A})}}\Delta[\ell] + \sum_{v=1}^{M} n_{s,v} \right\}. \quad (13) \end{aligned}$$

Assume that the MAI can be approximated by a zero mean Gaussian distributed random variable. Then the decision variable $Y_{o,s}$ normalized by $\sqrt{P_o/2M}T_o$ is modelled by a Gaussian random variable with mean

$$E[Y_{o,s}] = b_{o,s}[0]\sum_{v=1}^{M}|\alpha_{s,v}|^2 \quad (14)$$

and variance

$$\begin{aligned} Var[Y_{o,s}] &= \sum_{v=1}^{M}\sum_{k=1}^{K_{\mathbf{A}}}\sum_{\ell=0}^{L_k^{(\mathbf{A})}-1} Var\left[\sqrt{\frac{P_k^{(\mathbf{A})}}{P_o}}\frac{|\alpha_{s,v}|^2 c_k^{(\mathbf{A})}[v]c_o[v]}{L_k^{(\mathbf{A})}} \times \right. \\ &\quad \left. \Delta[\ell] + \frac{1}{2}\left(\frac{E_o}{MN_0}\right)^{-1}\sum_{v=1}^{M}|\alpha_{s,v}|^2 \right] \\ &= \sum_{v=1}^{M}\sum_{k=1}^{K_{\mathbf{A}}}\sum_{\ell=0}^{L_k^{(\mathbf{A})}-1} \frac{P_k^{(\mathbf{A})}}{P_o}\frac{|\alpha_{s,v}|^4}{(L_k^{(\mathbf{A})})^2} + \\ &\quad \frac{1}{2}\left(\frac{E_o}{MN_0}\right)^{-1}\sum_{v=1}^{M}|\alpha_{s,v}|^2 \ . \quad (15) \end{aligned}$$

Define the received E_b/N_0 (denoted by γ) as (16), where R_o and $R_k^{(\mathbf{A})}$ are the transmission rates of the reference user and user k in group $\mathbf{A}$, respectively. Note that E_o/N_0 denotes the reference user's transmitting signal-to-noise ratio per bit. $E_o = P_oT_o$ and $N_0 = P_NT_c$, where P_o and P_N are the transmission power of the reference user and the noise power. As in [14], [20], [21], $R_k^{(\mathbf{A})}/R_o = P_k^{(\mathbf{A})}/P_o$. That is, a high-rate user needs more power.

C. MAI Coefficient

In order to quantize the MAI imposed on each code channel, we define a new performance metric — *MAI coefficient*. In the considered single cell in downlink transmissions, all the interferers experience the same fading channel as the reference user. The only difference between these interferers are the volumes of interference they produce. Now, lets rewrite the MAI term of γ in (16) as

$$\sum_{k=1}^{K_{\mathbf{A}}}\sum_{\ell=0}^{L_k^{(\mathbf{A})}-1}\frac{R_k^{(\mathbf{A})}}{R_o(L_k^{(\mathbf{A})})^2}\left[2P_oG_o\sum_{v=1}^{M}|\alpha_{s,v}|^4\right] . \quad (17)$$

As shown in (17), the effects of the channel from other users will not contribute to the MAI imposed on the desired user. Since the downlink MAI is resulted from the subcarriers of reusing time-domain spreading codes in different frequency-domain code trees, we assume that the fading parameters in (17) are independent. With respect to the target user, the term $2P_oG_o\sum_{v=1}^{M}|\alpha_{s,v}|^4$ in (17) is common to all the $K_{\mathbf{A}}$ interfering users. As a result, we can just use $\sum_{k=1}^{K_{\mathbf{A}}}\sum_{\ell=0}^{L_k^{(\mathbf{A})}-1} R_k^{(\mathbf{A})}/(R_o(L_k^{(\mathbf{A})})^2)$ to characterize the downlink MAI in the MC-DS-CDMA system. There are two possible scenarios as described below.

1) **MAI from High Data Rate Users:** In this case $R_k^{(\mathbf{A})}/R_o = T_o/T_k^{(\mathbf{A})} = L_k^{(\mathbf{A})} > 1$. Then it follows that

$$\sum_{k=1}^{K_{\mathbf{A}}}\sum_{\ell=0}^{L_k^{(\mathbf{A})}-1}\frac{R_k^{(\mathbf{A})}}{R_o(L_k^{(\mathbf{A})})^2} = \sum_{k=1}^{K_{\mathbf{A}}}\sum_{\ell=0}^{L_k^{(\mathbf{A})}-1}\frac{1}{L_k^{(\mathbf{A})}} = \sum_{k=1}^{K_{\mathbf{A}}}1. \quad (18)$$

2) **MAI from Low Data Rate Users:** By letting $L_k^{(\mathbf{A})} = 1$ in (17), we can obtain the MAI from low data rate users as

$$\sum_{k=1}^{K_{\mathbf{A}}}\sum_{\ell=0}^{L_k^{(\mathbf{A})}-1}\frac{R_k^{(\mathbf{A})}}{R_o(L_k^{(\mathbf{A})})^2} = \sum_{k=1}^{K_{\mathbf{A}}}\frac{R_k^{(\mathbf{A})}}{R_o} . \quad (19)$$

Note that $R_k^{(\mathbf{A})}/R_o < 1$ in this case.

Combining (18) and (19), we define the downlink *MAI coefficient* in the MC-DS-CDMA system with TF-domain spreading as

$$\kappa = \sum_{k=1}^{K_{\mathbf{A}}}\mathbf{min}(1, \frac{R_k^{(\mathbf{A})}}{R_o}) \ . \quad (20)$$

According to the grid representation in Section II-C, (20) can also be expressed as

$$\kappa = \sum_{k=1}^{K_{\mathbf{A}}}\mathbf{min}(1, \frac{\sigma_k^{(\mathbf{A})}}{\sigma_o}) \ , \quad (21)$$

where $\sigma_k^{(\mathbf{A})}$ and σ_o represent the areas of the rectangles in Fig. 3 for codes with transmission rates $R_k^{(\mathbf{A})}$ and R_o, respectively. Note that referring to (17), the difference between the real MAI and its coefficient is $2P_oG_o\sum_{v=1}^{M}|\alpha_{s,v}|^4$.

V. Interference Avoidance Code Assignment Strategy

A. Principles

Now we propose an MAI-coefficient-based interference avoidance code assignment strategy. With the aid of the MAI coefficient, the proposed interference avoidance code assignment strategy can quickly and easily evaluate the candidacy of each spreading code and pick one which incurs less MAI. The objective of the interference avoidance code assignment

$$\gamma = \frac{E^2[Y_{o,s}]}{2Var[Y_{o,s}]} = \frac{(\sum_{v=1}^{M}|\alpha_{s,v}|^2)^2}{2\sum_{v=1}^{M}\sum_{k=1}^{K_{\mathbf{A}}}\sum_{\ell=0}^{L_k^{(\mathbf{A})}-1}\frac{P_k^{(\mathbf{A})}}{P_o}\frac{|\alpha_{s,v}|^4}{(L_k^{(\mathbf{A})})^2}+(\frac{E_o}{MN_0})^{-1}\sum_{v=1}^{M}|\alpha_{s,v}|^2} = \frac{P_oG_o(\sum_{v=1}^{M}|\alpha_{s,v}|^2)^2}{\underbrace{2\sum_{v=1}^{M}\sum_{k=1}^{K_{\mathbf{A}}}\sum_{\ell=0}^{L_k^{(\mathbf{A})}-1}\frac{P_k^{(\mathbf{A})}}{P_o}\frac{|\alpha_{s,v}|^4}{(L_k^{(\mathbf{A})})^2}P_oG_o}_{MAI}+\underbrace{MP_N\sum_{v=1}^{M}|\alpha_{s,v}|^2}_{noise}}, \quad (16)$$

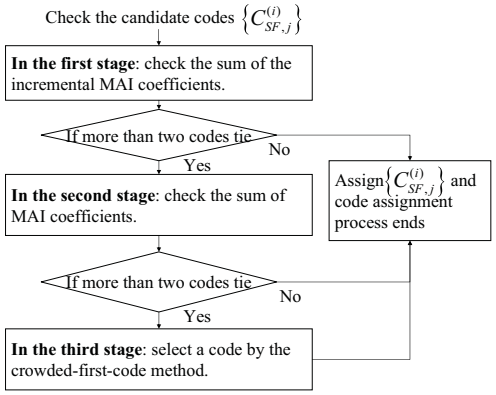

Fig. 6. Flow chart of the interference avoidance code assignment strategy.

strategy is to reduce the MAI effect in the MC-DS-CDMA system, while keeping the code tree compact to maintain low call blocking performance for users with various data rates. In principle, the proposed interference avoidance code assignment strategy consists of three stages. As shown in Fig. 6, the first stage is to check the sum of the incremental MAI coefficients of the candidate codes. If some candidate codes tie in the first stage, the sum of the MAI coefficients are compared. At last, the crowded-first code assignment in [9], [10] is applied for the candidate codes who tie in the second stage. The detail rules of the interference code assignment strategy are summarized as follows.

Let $\{C_{SF,j}^{(i)}\}$ be the set of candidate codes with frequency- and time-domain spreading factors M and SF, respectively, where $1 \le i \le M$ and $1 \le j \le SF$. Denote $\mathbf{R_c}(C_{SF,j}^{(i)})$ the set of the codes related to $C_{SF,j}^{(i)}$. The candidature of each code $C_{SF,j}^{(i)}$ is evaluated in the following three stages.

1) ***In the first stage***, the the incurred MAI of using code $C_{SF,j}^{(i)}$ is estimated by the sum of the increment of the MAI coefficients of codes in $\mathbf{R_c}(C_{SF,j}^{(i)})$. If any two candidate codes lead to the same amount of incremental MAI coefficients in $\mathbf{R_c}(C_{SF,j}^{(i)})$, go to the second stage. Otherwise, the smallest sum of incremental MAI coefficients in the set of $\mathbf{R_c}(C_{SF,j}^{(i)})$ is selected. We detail the rules in the first stage as follows:
   a) For the n-th code in $\mathbf{R_c}(C_{SF,j}^{(i)})$, denoted by $C_n \in \mathbf{R_c}(C_{SF,j}^{(i)})$, we calculate its increments of the MAI coefficient ($\Delta_\kappa(C_n)$) if $C_{SF,j}^{(i)}$ is chosen.
   b) Denote $\Delta_\kappa(\mathbf{R_c}(C_{SF,j}^{(i)}))$ the sum of $\Delta_\kappa(C_n)$ for $C_n \in \mathbf{R_c}(C_{SF,j}^{(i)})$. Then we can have
$$\Delta_\kappa(\mathbf{R_c}(C_{SF,j}^{(i)})) = \sum_{C_n \in \mathbf{R_c}(C_{SF,j}^{(i)})} \Delta_\kappa(C_n) \ . \quad (22)$$
   c) Select the codes with $\mathbf{min}\left\{\Delta_\kappa(\mathbf{R_c}(C_{SF,j}^{(i)}))\right\}$.
   d) If there is only one code with $\mathbf{min}\left\{\Delta_\kappa(\mathbf{R_c}(C_{SF,j}^{(i)}))\right\}$, the code assignment process ends, otherwise go to the next stage.
2) ***In the second stage***, the sum of the MAI coefficients of the codes in $\mathbf{R_c}(C_{SF,\beta}^{(\alpha)})$ are compared, where $\{C_{SF,\beta}^{(\alpha)}\}$ is the code set with the same sum of increment of MAI coefficients. In this stage, we assign the code with the smallest sum of MAI coefficients. If two candidates tie, go to the the third stage. The details of the rules in the second stage is as follows:
   a) Similar to the first step, we calculate the MAI coefficient of the n-th codes in $\mathbf{R_c}(C_{SF,\beta}^{(\alpha)})$, which is denoted by $\kappa(C_n)$.
   b) Denote $\kappa(\mathbf{R_c}(C_{SF,\beta}^{(\alpha)}))$ the sum of $\kappa(C_n)$, where $C_n \in \mathbf{R_c}(C_{SF,\beta}^{(\alpha)})$. Then we can have
$$\kappa(\mathbf{R_c}(C_{SF,\beta}^{(\alpha)})) = \sum_{C_n \in \mathbf{R_c}(C_{SF,\beta}^{(\alpha)})} \kappa(C_n) \ . \quad (23)$$
   c) Pick the codes with $\mathbf{min}\left\{\kappa(\mathbf{R_c}(C_{SF,\beta}^{(\alpha)}))\right\}$.
   d) If there is only one code with $\mathbf{min}\left\{\kappa(\mathbf{R_c}(C_{SF,\beta}^{(\alpha)}))\right\}$, the code assignment process ends, otherwise go to the last stage.
3) ***In the third stage***, a code in $\left\{C_{SF,\delta}^{(\gamma)}\right\}$ is selected according to the crowded-first-code principle as suggested in [10], where $\left\{C_{SF,\delta}^{(\gamma)}\right\}$ is the code set with the same sum of MAI coefficients in the second stage.

B. Example

Now we give an example to illustrate the interference avoidance code assignment strategy. Consider codes $\left\{C_{8,8}^{(1)}, C_{8,1}^{(3)}, C_{8,5}^{(4)}, C_{8,7}^{(4)}\right\}$ to be the representatives of their respective groups of the 2D code tree in Fig. 2. In other words, the MAI coefficients of codes within a group are the same.

1) Compare the increment of the MAI coefficient ($\sum \Delta_\kappa(\cdot)$): First, we compare the increment of the MAI coefficient $\sum \Delta_\kappa(\cdot)$. Referring to Fig. 3 and the definition of (1),

one can easily find that the related codes for code $C_{8,8}^{(1)}$ are $C_{2,2}^{(2)}$ and $C_{2,2}^{(3)}$ because they are seated in the same column of the grid representation. Thus, we have

$$\mathbf{R}_c(C_{8,8}^{(1)}) = \left\{C_{8,8}^{(1)}, C_{2,2}^{(2)}, C_{2,2}^{(3)}\right\} \ . \tag{24}$$

Based on (21), the incurred MAI coefficient $\Delta_\kappa(\mathbf{R}_c(C_{8,8}^{(1)}))$ after allocating code $C_{8,8}^{(1)}$ is equal to

$$\begin{aligned}\Delta_\kappa(\mathbf{R}_c(C_{8,8}^{(1)})) &= \sum_{C_n \in \mathbf{R}_c(C_{8,8}^{(1)})} \Delta_\kappa(C_n) \\ &= \Delta_\kappa(C_{8,8}^{(1)}) + \Delta_\kappa(C_{2,2}^{(2)}) + \Delta_\kappa(C_{2,2}^{(3)}) \\ &= 2.5 \ , \end{aligned} \tag{25}$$

where

$$\begin{aligned}\Delta_\kappa(C_{8,8}^{(1)}) &= \mathbf{min}(1, \frac{\sigma_{2,2}^{(2)}}{\sigma_{8,8}^{(1)}}) + \mathbf{min}(1, \frac{\sigma_{2,2}^{(3)}}{\sigma_{8,8}^{(1)}}) \\ &= \mathbf{min}(1, \frac{4}{1}) + \mathbf{min}(1, \frac{4}{1}) = 2 \ , \end{aligned} \tag{26}$$

$$\Delta_\kappa(C_{2,2}^{(2)}) = \mathbf{min}(1, \frac{\sigma_{8,8}^{(1)}}{\sigma_{2,2}^{(2)}}) = \frac{1}{4} \tag{27}$$

and

$$\Delta_\kappa(C_{2,2}^{(3)}) = \mathbf{min}(1, \frac{\sigma_{8,8}^{(1)}}{\sigma_{2,2}^{(3)}}) = \frac{1}{4} \ . \tag{28}$$

Similarly, we can obtain $\Delta_\kappa(\mathbf{R}_c(C_{8,1}^{(3)})) = 2.5$, $\Delta_\kappa(\mathbf{R}_c(C_{8,5}^{(4)})) = 4$, and $\Delta_\kappa(\mathbf{R}_c(C_{8,7}^{(4)})) = 4.25$. Since $\Delta_\kappa(\mathbf{R}_c(C_{8,8}^{(1)})) = \Delta_\kappa(\mathbf{R}_c(C_{8,1}^{(3)})) = 2.5$, the code assignment enters the second stage to compare codes $C_{8,8}^{(1)}$ and $C_{8,1}^{(3)}$.

2) Compare the sum of MAI coefficient ($\sum \kappa(\cdot)$): In this stage, the sum of MAI coefficients of related codes $\sum \kappa(\cdot)$ for codes $C_{8,8}^{(1)}$ and $C_{8,1}^{(3)}$ are compared.

   a) Calculate $\kappa(\mathbf{R}_c(C_{8,8}^{(1)}))$: Recall (24) that $\mathbf{R}_c(C_{8,8}^{(1)}) = \left\{C_{8,8}^{(1)}, C_{2,2}^{(2)}, C_{2,2}^{(3)}\right\}$. As shown in Fig. 3, $C_{4,3}^{(1)}$, $C_{8,7}^{(1)}$, $C_{8,8}^{(1)}$, and $C_{2,2}^{(3)}$ are positioned in the same column as $C_{2,2}^{(2)}$. Thus, we have $\mathbf{R}_c(C_{2,2}^{(2)}) = \left\{C_{2,2}^{(2)}, C_{4,3}^{(1)}, C_{8,7}^{(1)}, C_{8,8}^{(1)}, C_{2,2}^{(3)}\right\}$. Similarly, we can obtain $\mathbf{R}_c(C_{2,2}^{(3)}) = \mathbf{R}_c(C_{2,2}^{(2)})$. Then, it follows that

$$\begin{aligned}\kappa(\mathbf{R}_c(C_{8,8}^{(1)})) &= \sum_{C_n \in \mathbf{R}_c(C_{8,8}^{(1)})} \kappa(C_n) \\ &= \kappa(C_{8,8}^{(1)}) + \kappa(C_{2,2}^{(2)}) + \kappa(C_{2,2}^{(3)}) \\ &= 6 \ , \end{aligned} \tag{29}$$

   where $\kappa(C_{8,8}^{(1)})) = \Delta_\kappa(C_{8,8}^{(1)})) = 2$ from (25) and

$$\begin{aligned}\kappa(C_{2,2}^{(2)}) &= \kappa(C_{2,2}^{(3)}) \\ &= \mathbf{min}(1, \frac{\sigma_{4,3}^{(1)}}{\sigma_{2,2}^{(2)}}) + \mathbf{min}(1, \frac{\sigma_{8,7}^{(1)}}{\sigma_{2,2}^{(2)}}) + \\ &\quad \mathbf{min}(1, \frac{\sigma_{8,8}^{(1)}}{\sigma_{2,2}^{(2)}}) + \mathbf{min}(1, \frac{\sigma_{2,2}^{(3)}}{\sigma_{2,2}^{(2)}}) \\ &= \mathbf{min}(1, \frac{2}{4}) + \mathbf{min}(1, \frac{1}{4}) + \\ &\quad \mathbf{min}(1, \frac{1}{4}) + \mathbf{min}(1, \frac{4}{4}) = 2 \ . \end{aligned} \tag{30}$$

   b) Calculate $\kappa(\mathbf{R}_c(C_{8,1}^{(3)}))$:
   Referring to Fig. 3, it is clearly that

$$\begin{aligned}\mathbf{R}_c(C_{2,1}^{(2)}) &= \mathbf{R}_c(C_{2,1}^{(1)}) = \mathbf{R}_c(C_{8,1}^{(3)}) \\ &= \left\{C_{8,1}^{(3)}, C_{2,1}^{(1)}, C_{2,1}^{(2)}\right\} \ . \end{aligned} \tag{31}$$

   By the same approach of obtaining (29), we have

$$\begin{aligned}\kappa(\mathbf{R}_c(C_{8,1}^{(3)})) &= \sum_{C_n \in \mathbf{R}_c(C_{8,1}^{(3)})} \kappa(C_n) \\ &= \kappa(C_{8,1}^{(3)}) + \kappa(C_{2,1}^{(1)}) + \kappa(C_{2,1}^{(2)}) \\ &= 4.5 \ , \end{aligned} \tag{32}$$

   where $\kappa(C_{8,1}^{(3)})) = \Delta_\kappa(C_{8,1}^{(3)})) = 2$ and

$$\begin{aligned}\kappa(C_{2,1}^{(2)}) &= \kappa(C_{2,1}^{(1)}) \\ &= \mathbf{min}(1, \frac{\sigma_{8,1}^{(3)}}{\sigma_{2,1}^{(1)}}) + \mathbf{min}(1, \frac{\sigma_{2,1}^{(2)}}{\sigma_{2,1}^{(1)}}) \\ &= \mathbf{min}(1, \frac{1}{4}) + \mathbf{min}(1, \frac{4}{4}) = 1.25. \end{aligned} \tag{33}$$

   Since code $C_{8,1}^{(3)}$ will have less total MAI in the set of its related codes than code $C_{8,8}^{(1)}$, it is chosen to serve the requested call.

VI. Numerical Results

In this section, we illustrate the effectiveness of the proposed MAI-coefficient-based interference avoidance code assignment for the MC-DS-CDMA system. We first validate the correctness of Gaussian approximation of MAI. Then, we compare various code assignment strategies: random assignment (RM), pure crowded-first-code assignment (CF) without considering MAI, and the proposed interference avoidance assignment (IA+CF) methods.

A. Simulation Setup

1) Simulation Environment: In the simulation, we consider downlink MC-DS-CDMA in a single cell environment with the parameters listed in Table I. Based on the assumptions in [18], [19], the subcarriers carrying the same data bits are assumed to experience independent flat Rayleigh fading. The background noise is modelled by white Gaussian noise with double-sided power spectrum density of $N_0/2$ and the transmitting $E_b/N_0 = 12$ dB. A new call is modelled by a

Poisson arrival process with the arrival rate (λ) of $1/2$ per time unit and the departure rate (μ) selecting from the set $\{1/24,\ 1/32,\ 1/40,\ 1/48,\ 1/56,\ 1/64,\ 1/80,\ 1/96,\ 1/112,\ 1/128, 1/144, 1/160, 1/176\}$. Thus, there are $\lambda/\mu = 12 \sim 88$ active calls in the system on average. With $U = 128$ parallel substreams, the frequency domain spreading factor (M) is 8 and the time domain spreading factor (SF) are 4, 8, 16, or 32. Each call requests a code of $8R$ ($SF = 4$), $4R$ ($SF = 8$), $2R$ ($SF = 16$), or R ($SF = 32$) with a probability according to the code traffic pattern [a b c d], where R is the basic data rate and the code traffic pattern of [a b c d] means that the times of requesting data rates $8R$, $4R$, $2R$, and R are proportional to $a : b : c : d$, respectively. It is assumed that the data rate of each user is fixed during his call holding time. To quantify the total traffic load carried by the active calls with different data rates, we define an effective traffic load (ρ) as follows:

$$\rho = \frac{\lambda}{\mu} \times \frac{8R \times a + 4R \times b + 2R \times c + R \times d}{a + b + c + d} \times \frac{1}{32R} \quad , \quad (34)$$

where the time-domain spreading factor is selected from SF=[4 8 16 32] and the code traffic pattern of [a b c d] is already defined. For example, when $\lambda = 1/2$ and $\mu = 1/40$ and the code traffic pattern [1 1 2 8], the effective traffic load ρ is 125% of the utilization of the time-domain resources.

2) Call Admission Control Principle: For call admission control, we consider the average received E_b/N_0. For an MAI coefficient (κ), the average received E_b/N_0 can be calculated by taking the average of (35) over M subcarriers' fading channels. A new coming call is blocked if accepting this new call will decrease the signal quality of any active calls below the required received $E_b/N_o = 5$ dB. We simulate 10,000 incoming calls for each combination of λ and μ. The blocking rate is defined as the ratio of the number of blocked call to 10,000 incoming calls for all code assignment strategies considered in this paper.

3) Code Assignment Strategy: When a user requests a code with rate $2^k R$, a code assignment strategy should pick a free candidate code with rate $2^k R$ and ensure that its ancestor/decent codes are not used. In this paper, we compare our proposed IA+CF method with two other code assignment methods:

a) Random Assignment(RM): If there is one or more candidate codes in the 2D code tree, the RM method randomly selects a code without considering the code tree structure and impact of MAI.

b) Crowded-First(CF): If there is one or more candidate codes in the 2D code tree, the CF method picks a code whose ancestor code has the fewest free codes, thereby leaving more space for future high-rate users and so lowering the call blocking rate [10]. Note that the CF method considers the code tree structure but ignoring the impact of MAI.

B. Gaussian Approximation of MAI

To check the correctness of the Gaussian approximation of MAI, we simulate the MAI term $\sum_{v=1}^{M}\sum_{k=1}^{K_{\mathbf{A}}}\sum_{\ell=0}^{L_k^{(\mathbf{A})}-1}\sqrt{\frac{P_k^{(\mathbf{A})}}{P_o}}\frac{|\alpha_{s,v}|^2 c_k^{(\mathbf{A})}[v]c_o[v]}{L_k^{(\mathbf{A})}}\Delta[\ell]$ in (13). Fig. 7 presents an example of Gaussian approximation of MAI for the frequency-domain spreading factor $M = 8$. Let the time-domain spreading factor of both the reference user and single interferer be $SF = 16$. The statistics of the MAI are obtained from 10,000 simulations. As shown in the figure, the MAI in the MC-DS-CDMA system is close to a Gaussian distributed random variable because the decision variable of a desired signal is a combination of $M = 8$ subcarriers' signals and these eight subcarriers experience independent flat fading. This can justify the assumption used in our model for the MAI coefficient.

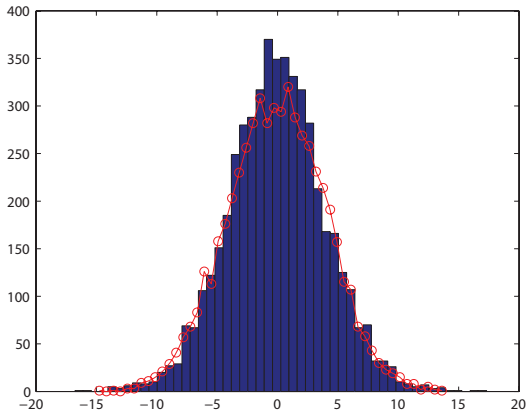

Fig. 7. An illustration example of approximating MAI by Gaussian distributed random variable. The time- and frequency-domain spreading factors of the reference and single interfering users are $SF = 16$ and $M = 8$, respectively.

C. Comparison of Code Assignment Strategies

Figs. 8(a) and 8(b) show the received E_b/N_0 and the call blocking rate of the RM, CF, and IA+CF code assignment strategies, with various effective traffic loads. We have following observations. First, comparing with RM, the IA+CF method has better received E_b/N_0 when $0.75 \le \rho \le 2.25$. However, for $\rho \ge 2.5$, IA+CF has lower received E_b/N_0 due to the increasing MAI by accommodating more users than RM. Second, comparing with CF, the IA+CF method has a better E_b/N_0 at the cost of a slightly higher call blocking rate. For $\rho = 2$, the E_b/N_0 improvement of the IA+CF method over the CF method is 1.9 dB, while the call blocking of IA+CF is 1.6% higher than CF. The reason why the call blocking rate for the IA+CF method is slightly higher than that of the CF method can be explained as follows. The CF method can make the tree structure of the allocated codes more compact to gather more larger code resources for higher-rate users, thereby lowering the blocking rate. The IA+CF method aims to avoid MAI first before executing the CF principle. Third, one can also find that for $1 \le \rho \le 2.25$, the IA+CF method has highest received E_b/N_0, the RM method ranks second, and the CF method has the lowest E_b/N_0. Fourth, as the traffic load increases, the difference between the IA+CF and CF methods in terms of both E_b/N_0 and blocking probability becomes smaller. For example, the difference of E_b/N_0 between two methods decreases from 1.9 to 0.1 dB as ρ changes from 2 to 5.5; the call blocking rate appears to be the same at

TABLE I
THE SIMULATION PARAMETERS

Call arrival rate (λ)	$1/2$
Departure rate (μ)	$\{1/24, 1/32, 1/40, 1/48, 1/56, 1/64, 1/80, 1/112, 1/128, 1/144, 1/160, 1/176\}$
Frequency-domain spreading factor (M)	8
Time-domain spreading factor (SF)	[4 8 16 32]
Code traffic pattern	[1 1 2 8]
Transmitting E_b/N_0	12 dB
Required received E_b/N_0	5 dB

$\rho = 5.5$. This is because when there are more active users in the system, the IA+CF method can not easily find a good code with low interference for a new coming user. In this situation, the IA+CF method picks a code according to the CF principle.

VII. CONCLUDING REMARKS

In this paper, we have proposed a novel interference avoidance code assignment strategy for multi-rate MC-DS-CDMA with TF-domain spreading. We analyze the error rate performance and defined new performance metric — *MAI coefficient* — to estimate the quantity of MAI imposed on each code channel. By simulations and analysis, we demonstrate that the proposed interference avoidance code assignment method can effectively reduce the MAI for multi-rate users in an MC-DS-CDMA system with time- and frequency-domain spreading, while maintaining the low call blocking rate. Interesting, future research topic is to apply the MAI coefficients to the MC-DS-CDMA system when combining power control mechanisms [22] or the multiple-input-multiple-out technology [23].

VIII. APPENDIX

In this Appendix, we use the Laguerre integration to evaluate the error rate performance of the synchronous multi-rate MC-DS-CDMA system with TF-domain spreading. Now, substituting the MAI coefficient κ of (20) into the received E_b/N_0 of (16), we obtain

$$\gamma = \left[\frac{2\sum_{v=1}^{M} |\alpha_{s,v}|^4}{(\sum_{v=1}^{M} |\alpha_{s,v}|^2)^2} \kappa + \frac{[E_o/(MN_o)]^{-1}}{\sum_{v=1}^{M} |\alpha_{s,v}|^2} \right]^{-1} . \quad (35)$$

For binary phase shift keying modulation with coherent detection, the conditional error probability for a given $\alpha_{s,v}$ is equal to

$$P(e|\alpha_{s,1}, \cdots, \alpha_{s,M}) = Q(\sqrt{2\gamma}) , \quad (36)$$

where $Q(x) = \frac{1}{\sqrt{2\pi}} \int_x^\infty e^{-t^2/2} dt$. Since $|\alpha_{s,v}|$ is the amplitude of the Rayleigh fading channel, $|\alpha_{s,v}|^2$ is an exponentially distributed random variable with mean $E[|\alpha_{s,v}|^2] = 1$. To ease the notation, we denote $z_v = |\alpha_{s,v}|^2$. Then the probability density function (*pdf*) of z_v is expressed as

$$f_{z_v}(z_v) = e^{-z_v} U(z_v), \quad (37)$$

where

$$U(t) = \begin{cases} 1, & t \geq 0 , \\ 0, & t < 0 . \end{cases} \quad (38)$$

Hence, the total error probability can be expressed as

$$\begin{aligned} P(e) &= \int_0^\infty \cdots \int_0^\infty Q(\sqrt{2\gamma}|z_1, \cdots, z_M) \times \\ &\quad f_{z_1}(z_1) \cdots f_M(z_M) dz_1 \cdots dz_M \\ &= \int_0^\infty \cdots \int_0^\infty Q(\sqrt{2\gamma}|z_1, \cdots, z_M) \times \\ &\quad e^{-z_1} \cdots e^{-z_M} dz_1 \cdots dz_M . \end{aligned} \quad (39)$$

Based on the Laguerre polynomial approach of [24], the integration for a function $q(x)e^{-x}$ can be computed by

$$\int_0^\infty q(x) e^{-x} dx = \sum_{i=1}^{H} \omega_i q(x_i) , \quad (40)$$

where x_i and ω_i are the abscissas and the weight factor of the Laguerre polynomials with order H, respectively. Applying the Laguerre integration into (39), we can further simplify the total error probability $P(e)$ to

$$\begin{aligned} P(e) &= \sum_{i_1=1}^{H} \cdots \sum_{i_M=1}^{H} w_{1,i_1} \times \cdots \times w_{M,i_M} \times \\ &\quad Q(\sqrt{2\gamma}|z_{1,i_1}, \cdots, z_{M,i_M}) . \end{aligned} \quad (41)$$

REFERENCES

[1] F.-T. Chien, C.-H. Hwang, and C.-C. Kuo, "Analysis of asynchronous long-code multicarrier CDMA systems with correlated fading," *IEEE Trans. Commun.*, vol. 53, no. 4, pp. 666–676, Apr. 2005.

[2] S.-M. Tseng and M. R. Bell, "Asynchronous multicarrier DS-CDMA using mutually orthogonal complementary sets of sequences," *IEEE Trans. Commun.*, vol. 48, no. 1, pp. 53–59, Jan. 2000.

[3] H. Liu and H. Yin, "Recevier design in multicarrier direct-sequence CDMA communications," *IEEE Trans. Commun.*, vol. 49, no. 8, pp. 1479–1487, Aug. 1997.

[4] S. Kondo and L. B. Milstein, "Performance of multicarrier CDMA systems," *IEEE Trans. Commun.*, vol. 44, no. 2, pp. 238–246, Feb. 1996.

[5] D. K. Kim and S.-H. Hwang, "Capacity analysis of an uplink synchronized multicarrier DS-CDMA system," *IEEE Commun. Lett.*, vol. 6, no. 3, pp. 99–101, Mar. 2002.

[6] L.-L. Yang and L. Hanzo, "Performance of generalized multicarrier DS-CDMA over Nagagami-m fading channels," *IEEE Trans. Commun.*, vol. 50, no. 6, pp. 956–966, June 2002.

[7] C. W. You and D. S. Hong, "Multicarrier CDMA systems using time-domain and frequency-domain spreading codes," *IEEE Trans. Commun.*, vol. 51, no. 1, pp. 17–21, Jan. 2003.

[8] C.-M. Yang, P.-H. Lin, G.-C. Yang, and W. C. Kwong, "2D orthogonal spreading codes for multicarrier DS-CDMA systems," in *Proc. IEEE ICC*, May 2003, vol. 5, pp. 3277–3281.

[9] Y.-C. Tseng and C.-M. Chao, "Code placement and replacement strategies for wideband CDMA OVSF code tree management," in *Proc. IEEE Trans. Mobile Computing*, vol. 1, no. 4, pp. 293–302, Oct.-Dec. 2002.

[10] Y.-C. Tseng, C.-M. Chao, and L.-C. Wang, "Reducing internal and external fragmentations of OVSF codes in WCDMA systems with multiple codes," *IEEE Wireless Commun. Networking Conf.*, Mar. 2003, vol. 1, pp. 693–698.

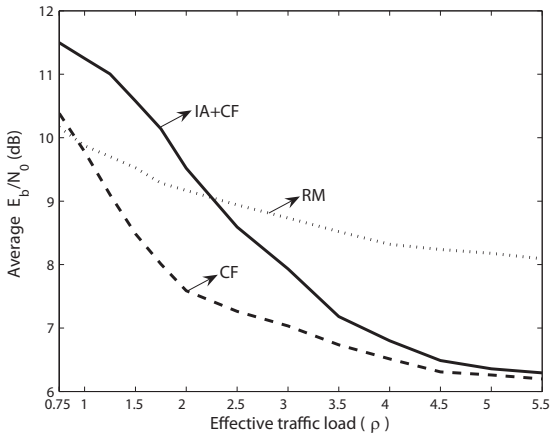

(a) Average received E_b/N_0 (dB)

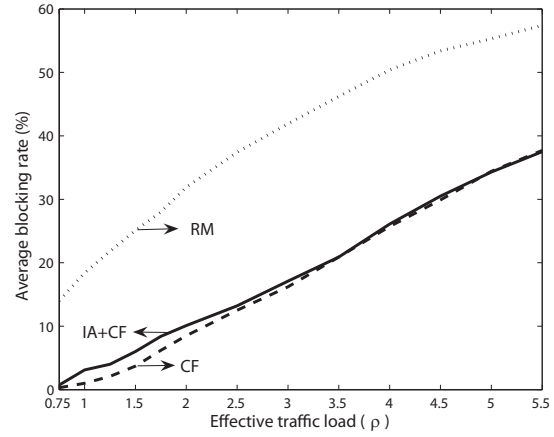

(b) Average blocking rate

Fig. 8. Comparison of the average received E_b/N_0 and call blocking rate against the effective traffic load for the RM, CF, and the IA+CF code assignment strategies, where the code pattern is [1 1 2 8], $E_b/N_0 = 12$ dB at the transmitter, and the required received $E_b/N_0 = 5$ dB.

[11] M. D. Amico, F. Maffioli, and M. L. Merani, "A tree partitioning dynamic policy for OVSF codes assignment in wideband CDMA," *IEEE Trans. Wireless Commun.*, vol. 3, no. 4, pp. 1013–1017, July 2004.

[12] H. Wei, L.-L. Yang, and L. Hanzo, "Time- and frequency-domain spreading assisted MC-DS-CDMA using interference rejection spreading codes for quasi-synchronous communications," in *Proc. IEEE Veh. Technol. Conf.*, Sep. 2004, vol. 1, pp. 389–393.

[13] ——, "Interference-free broadband single-and multicarrier DS-CDMA," *IEEE Commun. Mag.*, vol. 43, no. 2, pp. 68–73, Feb. 2005.

[14] M. Amadei, U. Manzoli, and M. Merani, "On the assignment of walsh and quasi-orthogonal codes in a multicarrier DS-CDMA system with multiple classes of users," in *Proc. IEEE Globecom*, Nov. 2002, vol. 1, pp. 841–845.

[15] U. Manzoli and M. Merani, "Multicarrier DS-CDMA performance with different assignment strategies of quasi-orthogonal codes," in *Proc. IEEE International Symposium Pers., Indoor Mobile Radio Commun.*, Sep. 2002, vol. 4, pp. 1477–1481.

[16] S. Sureshkumar, E. Shwedyk, and H. H. Nguyen, "MAI-minimized signature waveforms for MC-DS-CDMA systems," in *Proc. IEEE Veh. Technol. Conf.*, June 2005, vol. 1, pp. 305–309.

[17] H. Holma and A. Toskala, *WCDMA for UMTS: Radio Access for Third Generation Mobile Communications*, 2nd ed. New York: John Wiley & Sons, Ltd., 2002.

[18] L.-C. Wang and C.-W. Chang, "Performance analysis of multicarrier DS-CDMA with imperfect power control and variable spreading factors," in *Proc. IEEE Global Telecommun. Conf.*, Nov. 2005, vol. 6, pp. 3897–3901.

[19] L.-L. Yang and L. Hanzo, "Multicarrier DS-CDMA: A multiple access scheme for ubiquitous broadband wireless communications," *IEEE Commun. Mag.*, vol. 41, no. 10, pp. 116–124, Oct. 2003.

[20] K. S. Lim and J. H. Lee, "Performance of multirate transmission schemes for a multicarrier DS/CDMA system," in *Proc. IEEE Veh. Technol. Conf.*, Oct. 2001, vol. 2, pp. 767–771.

[21] T. Ottosson and A. Svensson, "On schemes for multirate support in DS-CDMA systems," *IEEE Wireless Pers. Commun.*, vol. 6, no. 3, pp. 265–287, Mar. 1998.

[22] Y. Zhu and E. Gunawan, "Performance of MC-CDMA system using controlled MRC with power control in Rayleigh fading channel," *IEE Electron. Lett.*, vol. 36, no. 8, pp. 752–753, Apr. 2000.

[23] C. S. Park and K. B. Lee, "Transmit power allocation for BER performance improvement in multicarrier systems," *IEEE Trans. Commun.*, vol. 52, no. 10, pp. 1658–1663, Oct. 2004.

[24] M. Abramowitz and I. A. Stegun, "Handbook of mathematical functions with formulas, graphs, and mathematical tables," *U.S. Department of Commerce National Bureau of Standards Applied Mathematics Series 55*, 1964.

Li-Chun Wang received the B.S. degree from National Chiao Tung University , Taiwan, R. O. C. in 1986, the M.S. degree from National Taiwan University in 1988, and the Ms.Sci. and Ph.D. degrees from the Georgia Institute of Technology, Atlanta, in 1995, and 1996, respectively, all in electrical engineering.

From 1990 to 1992, he was with the Telecommunications Laboratories of the Ministry of Transportations and Communications in Taiwan (currently the Telecom Labs of Chunghwa T elecom Co.). In 1995, he was affiliated with Bell Northern Research of Northern Telecom, Inc., Richardson, TX. From 1996 to 2000, he was a Senior Technical Staff Member in the Wireless Communications Research Department of AT&T Labs- Research. Since August 2000, he has been an Associate Professor in the Department of Communication Engineering of National Chiao Tung University in Taiwan and become a full processor in Aug. 2005. His current research interests are in the areas of adaptive/cognitive wireless networks, radio network resource management, cross-layer optimization, and cooperative wireless communications networks..

Dr. Wang was a co-recipient (with Gordon L. Stüber and Chin-Tau Lea) of the Jack Neubauer Best Paper Award of the IEEE Vehicular Technology Society in 1997. He has published over 30 journal and 70 international conference papers and is holding three US patents. He served as an Associate Editor for the IEEE TRANSACTIONS ON WIRELESS COMMUNICATIONS from 2001 to 2005, the guest editor of the special issue on "Mobile Computing and Networking" for the IEEE JOURNAL ON SELECTED AREAS IN COMMUNICATIONS in 2005 and the special issue on "Radio Resource Management and Protocol Engineering in Future IEEE Broadband Networks" for *IEEE Wireless Communications Magazine* in 2006.

Chih-Wen Chang received the BS and MS degrees in electrical engineering from National Sun Yat-Sen University, Kaohsiung, Taiwan, in 1998 and 2000, respectively. He obtained the Minor MS degree in applied mathematics and the PhD degree in communication engineering from National Chiao-Tung University HsinChu, Taiwan, in 2005 and 2006, respectively. He was awarded the IEEE student travel grant for ICC 2006 and the membership of the Phi Tau Phi scholastic honor society in 2006. Since August 2006, he has been an assistant professor in the Institute of Computer and Communication Engineering at National Cheng Kung University in Taiwan. His current research interests include wireless communications, wireless networks, and cross-layer design.

Howard Huang received a B.S. in Electrical Engineering (1991) from Rice University and a Ph.D. in Electrical Engineering (1995) from Princeton University. Since then, he has been a researcher at Bell Labs (Alcatel-Lucent) in Holmdel, New Jersey, currently as a Distinguished Member of Technical Staff in the Broadband and Wireless Access Center. His interests are in MIMO techniques and their application in practical cellular networks. He is currently a guest editor for a JSAC issue on MIMO for next-generation wireless systems.